

Prediction of Sound Absorption Coefficient by Applying Various Models

Aleksandar Pantić, Dejan Ćirić, *ETAN Member*, Maro Puljizević, and Marko Janković, *ETAN Member*

Abstract—Sound absorption coefficient can be obtained either by measurements or by prediction using different models. Some of them are based on empirical data, while some others are based on theoretical considerations of sound propagation within absorbing materials. Although a number of studies deal with limitations and performance of the predictive models, it is still not completely clear how accurate and useful these models are in everyday practice. This paper analyzes several empirical and semi-phenomenological models for prediction of sound absorption coefficient of rock mineral wool materials. Focus is on the effects of changing the input data (parameters) needed to apply the models. Some of the input parameters are obtained in the measurements, like airflow resistivity and thickness, while other input data are taken from the literature. For two particular cases, the predicted results are compared to the absorption coefficient measured in the impedance tube.

Index Terms—Sound absorption coefficient, prediction models, empirical data, phenomenological analysis, accuracy.

I. INTRODUCTION

MEASUREMENTS in the field of noise engineering that include obtaining the absorption coefficient can be extremely expensive and in some cases time demanding. An alternative approach able to predict the results with acceptable degree of accuracy would be of significant importance [1]. Thus, it would be beneficial to have a modeling tool that enables evaluation of performance of sound absorbing materials.

During previous decades, various models have become available providing parameters that can be used to characterize various types of absorbents and that are capable of physical interpretation [2]. One way how the acoustical properties of absorbing materials can be described is by using the characteristic acoustic impedance and propagation constant [3,4]. Based on these two quantities, the normal incidence absorption for a particular thickness and mounting arrangement can be derived [4].

According to the nature of the models used for predicting

Aleksandar Pantić is with the Knauf Insulation d.o.o., Serbia, Batajnički drum 16b, 11090 Belgrade, Serbia, (e-mail: aleksandar.pantic@knaufinsulation.com).

Dejan Ćirić is with the University of Niš, Faculty of Electronic Engineering in Niš, Aleksandra Medvedeva 14, 18000 Niš, Serbia (e-mail: dejan.ciric@elfak.ni.ac.rs), ORCID ID (<https://orcid.org/0000-0003-4974-3131>).

Maro Puljizević is with the Knauf Insulation d.o.o., Slovenia, Trata 32, SI-4220 Škofja Loka, Slovenia, (maro.puljizevic@knaufinsulation.com).

Marko Janković is with the University of Niš, Faculty of Electronic Engineering in Niš, Aleksandra Medvedeva 14, 18000 Niš, Serbia (e-mail: marko.p.jankovic@elfak.rs), ORCID ID (<https://orcid.org/0009-0002-1109-3241>).

acoustical behavior of porous materials, they may be classified in one of two categories: empirical and theoretical (semi-phenomenological) micro-structural models [5-7]. Here, the empirical models are developed by applying certain regression relations to a number of measurement results of particular materials (typically of the impedance and airflow resistivity) [8]. Consequently, there are different empirical models for different material types [6]. On the other hand, the theoretical models are developed by physical considerations of sound propagation in materials using more complex independent variables, such as tortuosity and porosity [6]. Structural and geometrical complexities represent significant drawbacks of theoretical models in describing the acoustical behavior of most sound absorbers [5]. This is why empirical models have had a significant role for the mentioned task [5].

Among empirical models, one of the most used one is the model proposed by Delany and Bazely (DB model). [5] This model based on simple power-law relations was obtained by best fitting the large amount of experimental data to the analytical expression leading to particular values of coefficients (model parameters) [2,5,7].

Several researchers have proposed modified versions of the DB model, such as Bies and Hansen, Miki or Davern and Dunn [5,8]. Even neural networks were used to implement an empirical model for polyurethane foams with a single input parameter, again the airflow resistivity [9]. In some other modifications of the DB model, its parameters were updated for a particular type of material, that is, the material specific models were developed [1]. Thus, the modification of DB model was proposed by Garai and Pompoli (GP) for materials made of polyester fibers [9].

A generalized model not only developed for a particular type of material was proposed by Johnson, Champoux and Allard (JCA) [5]. This JCA model has five input parameters: airflow resistivity, porosity, tortuosity, viscous and thermal characteristic lengths [5]. The former two of these parameters (airflow resistivity and porosity) can directly be measured, while the other three parameters are more complex to be obtained [5]. The JCA model has proved particularly good at low frequencies [8].

Prediction accuracy of the available models has been investigated in the literature, however, it is still not completely clear which is the best model for a particular use-case. It is stated that prediction accuracy of the existing models is almost unknown in scientific terms leading to a serious gap in the knowledge [6]. A solution could be to select a model based on the distinctive absorption mechanism and

type of porosity of the analyzed material [8].

This paper analyzes the performance of several models for absorption coefficient prediction. The input data required for these models are either obtained by direct measurements, such as airflow resistivity, or by apriori knowledge of acoustical behavior or rock mineral wool materials. The effects of changing the input parameter (airflow resistivity) are observed. The results obtained by modeling are compared with the ones obtained by the measurements in the impedance tube.

II. MODELS USED IN THIS STUDY

A. Delany – Bazley Model

The DB model is basically a single parameter model in which the characteristic impedance and propagation constant (coefficient) of the material is predicted using only the static airflow resistivity. This model is considered as an easy and relatively accurate model, which is primarily empirical, but loosely based on theory [4]. Such a model takes a macroscopic view and the details of the propagation through pores are not considered [7]. In this way, microscopic properties of an absorber, such as the pore size and orientation of the pores, are not taken into account.

In the DB model, the characteristic impedance Z_c can be represented as [2,10]:

$$Z_c = R + jX = Z_0 \left[1 + C_1 \left(\frac{\rho_0 f}{\sigma} \right)^{-C_2} - jC_3 \left(\frac{\rho_0 f}{\sigma} \right)^{-C_4} \right], \quad (1)$$

where the constants are given as $C_1 = 0.0571$, $C_2 = 0.754$, $C_3 = 0.087$ and $C_4 = 0.732$, $Z_0 = \rho_0 c_0$ is the characteristic impedance of air, ρ_0 is the air density at room temperature ($\approx 1.2 \text{ kg/m}^3$), f is the frequency, σ is the airflow resistivity (rayl/m), c_0 is the speed of sound in air at room temperature ($\approx 343 \text{ m/s}$). In the same way, the propagation constant is defined as [2,10]

$$\Gamma = \alpha + j\beta = \frac{\omega}{c_0} \left[1 + C_5 \left(\frac{\rho_0 f}{\sigma} \right)^{-C_6} - jC_7 \left(\frac{\rho_0 f}{\sigma} \right)^{-C_8} \right], \quad (2)$$

where the constant are $C_5 = 0.0978$, $C_6 = 0.7$, $C_7 = 0.189$, and $C_8 = 0.595$, $k_0 = \omega/c_0 = 2\pi f/c_0$ is the free field wave-number.

By using the obtained values of the characteristic impedance and propagation constant, the normal incidence sound absorption coefficient can be obtained as [9,10]

$$a = \frac{4Z_{sr}Z_0}{|Z_s|^2 + 2Z_0Z_{sr} + Z_0^2}, \quad (3)$$

where Z_s is the rigid-backing specific surface impedance given as a function of the material layer thickness d [10]

$$Z_s = Z_{sr} + jZ_{si} = Z_c \coth(\Gamma d), \quad (4)$$

Since the DB model uses a very simple single power-law relations, it can be expected that they are not able to provide a perfect fit with the measured data, but still can provide a reasonably good prediction values [3]. The DB model can be

used with confidence within the interpolating range, which is $0.01 \leq f/\sigma \leq 1$ [6,10]. However, for some materials, the stated condition is not fulfilled at low frequencies (below 250 Hz). Outside of the interpolating range, that is, at low frequencies, it can happen that the DB model results in a negative impedance, which is not physically realizable solution. Another assumed condition in DB model is that the porosity of the material should be very close to unity. Fortunately, most purpose-built fibrous absorbers achieve this condition [7].

B. Mechel – Grundmann Model

The empirical equations obtained by a regression process are combined with an analytical approximation for low frequencies in the Mechel model [6]. However, as a consequence of transition from the analytical to the empirical equations, there are discontinuity points in the predicted absorption coefficient. In the revised Mechel model, the analytical approximation is ignored, but two sets of coefficients are introduced – one for low frequencies and another for high frequencies [6]. The accuracy of results obtained by this method is satisfactory above 400 Hz [6].

Mechel and Grundmann model (MG model), representing one of the modifications of the DB model, consists of a more complex set of empirical relationships given as [7]

$$\left. \begin{aligned} \frac{jk/k_0}{Z_n} \right\} &= X^{-1}\beta_{-1} + X^{-1/2}\beta_{-1/2} + \\ &\beta_0 + X^{1/2}\beta_{1/2} + X^1\beta_1 + X^{3/2}\beta_{3/2} \end{aligned} \right\}, \quad (5)$$

where separate formulations were derived for mineral fibre and glass fibre. The coefficients for mineral fibre are summarized in Table I. The range of applicability of this model is $0.003 < (\rho_0 f/\sigma) < 0.4$ [7]. In spite of certain differences in formulations, the difference in the predicted quantities between DB and MG models is small for many materials.

TABLE I
COEFFICIENTS OF THE MG MODEL FOR POROUS ABSORBERS (MINERAL FIBER, E.G., BASALT OR ROCK WOOL)

Coefficients	$-jk/k_0$	Z_n
β_{-1}	-0.00355757 -j 0.0000164897	0.0026786 +j 0.00385761
$\beta_{1/2}$	0.421329 +j 0.342011	0.135298 -j 0.394160
β_0	-0.507733 +j 0.086655	0.946702 +j 1.47653
$\beta_{1/2}$	-0.142339 +j 1.25986	-1.45202 -j 4.56233
β_1	1.29048 -j 0.0820811	4.03171 +j 7.56031
$\beta_{3/2}$	-0.771857 -j 0.668050	-2.86993 -j 4.90437

Wilson Model

An alternative approach to modeling the propagation

through porous absorbing materials was applied in the development of the Wilson model. Here, the thermal and viscous diffusion are considered as relaxation processes [7]. This is based on the fact that when sound propagates through porous materials, the result is manifested in temperature perturbations within the air inside the absorbing material. Over time, these perturbations are relaxed towards the equilibrium temperature, where the characteristic time of the thermal relaxation process is denoted by τ_t . Similar situation is valid for the pressure gradients set up by the sound wave, inducing changes in the flow velocity that are also relaxed towards the steady state. This viscous relaxation process is described by its characteristic time denoted by τ_v . Now, the characteristic impedance and propagation constant in a relaxation form can be derived from the inverse of the bulk modulus and effective density as [7]

$$Z_c = \frac{\rho_0 c_0 \sqrt{\alpha_\infty}}{\phi} \left[\left(1 + \frac{\gamma - 1}{\sqrt{1 + j\omega\tau_t}} \right) \left(1 + \frac{1}{\sqrt{1 + j\omega\tau_v}} \right) \right]^{-0.5}, \quad (6)$$

$$k = \frac{\omega \sqrt{\alpha_s}}{c} \left[\left(1 + \frac{\gamma - 1}{\sqrt{1 + j\omega\tau_t}} \right) \right] / \left[\left(1 - \frac{1}{\sqrt{1 + j\omega\tau_v}} \right) \right]. \quad (7)$$

The appropriate choice of relaxation times lead to the results that match the empirical and semi-phenomenological models. For example, by setting the following values: $\tau_v = 2.54/\sigma$ and $\tau_t = 3.75/\sigma$, $\alpha_\infty = 1$ and $\varepsilon = 1$, the same predictions as by the DB model are obtained. This relaxation method does not offer any great advantages over other models, except that at low frequencies the acoustic parameters at low frequency are limited to correct physical values [7].

C. Johnson – Champoux – Allard Model

The JCA model is one of the semi-phenomenological models developed from theoretical considerations of the viscous forces in porous materials [6]. This model requires prediction of two quantities – dynamic density (that takes into account the inertial and viscous forces of the air in the material) and dynamic bulk modulus (takes into account the thermal exchanges between the air in pores and the rigid frame) [6]. The effective (dynamic) density $\rho_e(\omega)$ can be calculated as [7]

$$\rho_e = \frac{\alpha_\infty \rho_0}{\phi} \left[1 + \frac{\sigma \phi}{j\omega \rho_0 \alpha_\infty} \sqrt{1 + \frac{4j\alpha_\infty^2 \eta \rho_0 \omega}{\sigma^2 \Lambda^2 \phi^2}} \right], \quad (8)$$

while the dynamic bulk modulus is represented by [7]

$$K_e = \frac{\gamma P_0}{\phi} \left[\gamma - (\gamma - 1) \left/ \left(1 + \frac{8\eta}{j\Lambda^2 N_p \omega \rho_0} \sqrt{1 + \frac{j\rho_0 \omega N_p \Lambda^2}{16\eta}} \right) \right. \right]^{-1}, \quad (9)$$

where γ is the specific heat ratio (≈ 1.4), P_0 is the air equilibrium pressure $\approx 101,320 \text{ Nm}^{-2}$, and N_p is the Prandtl number defined by using viscous (δ_v) and thermal boundary layers (δ_t) as $N_p = (\delta_t/\delta_v)^2$ [7]. At the atmospheric pressure of

1 atmosphere and temperature of 20°C , the Prandtl number is about 0.77 [7]. The thicknesses of the mentioned viscous and thermal boundary layers are given by [7]

$$\delta_v = \sqrt{(2\eta)/(\rho_0\omega)} \quad \delta_t = \sqrt{(2\kappa)/(\rho_0 c_p \omega)}, \quad (10)$$

where $\kappa \approx 2.41 \times 10^{-2} \text{ WmK}^{-1}$ is the thermal conductivity of air, and $c_p \approx 1.01 \text{ Jkg}^{-1}\text{K}^{-1}$ is the specific heat of air at constant pressure [7]. The viscous boundary layer is typically submillimetre in size, e.g., it is about 0.2 mm at 100 Hz. The equations for the dynamic density and dynamic bulk modulus are derived under the hypothesis that the material tortuosity and porosity are very nearly unity, and they can be valid only at normal incidence [11].

Having those two quantities known and at normal incidence, the characteristic impedance Z_c and propagation constant Γ can be calculated as

$$Z_c = \sqrt{\rho_e K_e} \quad \Gamma = \omega \sqrt{\rho_e / K_e}. \quad (11)$$

The surface impedance of a rigidly backed layer and the normal-incidence energy absorption coefficient can be calculated by applying (3) and (4) [11].

To implement the semi-phenomenological model, the following assumptions are made: $\phi = 0.98$, $\alpha_\infty = 1$, $\Lambda' = \Lambda$, and $s = 1$. The JCA model sometimes produces errors in the estimation of the transition frequency between the isothermal and adiabatic regime, where thermal dissipation is at its greatest [7]. Fortunately, this is not problematic typically for conventional porous materials since the viscous effects normally dominate in these materials.

The equations of the JCA model yield the correct high and low frequency asymptotic behavior [7]. However, they are only approximately correct at mid frequencies for complicated pore geometries. The predictions obtained by the JCA and DB model are very similar in the range of validity of the latter model.

D. Johnson – Champoux – Allard – Lafarge Model

The Johnson – Champoux – Allard – Lafarge (JCAL) model was developed by including two additional parameters - the static thermal permeability (q_0') and the static viscous permeability (q_0) [7]. These two parameters can be either measured or predicted. Here, the subscript 0 indicates that these are the static values ($\lim \omega \rightarrow 0$), and the dash indicates it is a thermal value and the absence of the dash indicates a viscous value.

The dynamic viscous permeability q given by

$$q = q_0 \left(j \frac{\omega}{\omega_v} + \sqrt{1 + \frac{j\omega M_v}{\omega_v}} \right)^{-1}, \quad (12)$$

is used in the JCAL model, where ω_v is the viscous characteristic frequency and M_v is the viscous shape factor. These two parameters can be calculated as [7]

$$\omega_v = \frac{\eta\phi}{\alpha_\infty q_0 \rho_0} \quad M_v = \frac{8q_0 \alpha_\infty}{\phi \Lambda^2}. \quad (13)$$

The static viscous permeability, q_0 included in (12), is by definition given as $q_0 = \eta/\sigma$ [7]. As a consequence of the previously mentioned, the same parameters that are used in the JCA model are also applied in the JCAL model to represent the viscous effects [7]. On the other hand, the formulations for the dynamic thermal permeability, q' , in these two models are not the same, where the thermal formulations in the JCAL model are

$$q'(\omega) = q'_0 \left(j \frac{\omega}{\omega_t} + \sqrt{1 + \frac{j\omega M_t}{\omega_t}} \right)^{-1}, \quad (14)$$

where the thermal characteristic frequency (ω_t) and thermal shape factor (M_t) are given by

$$\omega_t = \frac{\kappa\phi}{c_p \rho_0 q'_0} \quad M_t = \frac{8q'_0}{\phi \Lambda^2}. \quad (15)$$

Based on the obtained thermal and viscous permeabilities, (14) and (12), the effective density and bulk modulus can be calculated by:

$$\rho_e = \frac{\eta}{j\omega q} \quad K_e = \frac{\gamma P_0}{\phi} \left(\gamma - (\gamma - 1) j\omega \rho_0 c_p \frac{q'}{\kappa\phi} \right)^{-1}. \quad (16)$$

The effective density has the same form in the JCAL model as in the JCA model.

III. METHODS OF INVESTIGATION

Three empirical models, DB, MG and Wilson model, as well as two semi-phenomenological models, JCA and JACL model, are used in this study for analyzing the results of absorption coefficient modeling. The former group of models is based on a single parameter – airflow resistivity, and this is why the effect of changing this parameter is investigated here. The other quantities necessary to make the modeling are the speed of sound at room temperature (343 m/s) and density of air at room temperature (1.204 kg/m^3). The thickness of the absorbing material is chosen to be 5 cm.

Taking into account diverse acoustic absorbing materials, the airflow resistivity can take value in a rather broad range from several thousands to several hundreds of thousands or even several millions of Nsm^{-4} . To cover the values that are typically found in the glass and rock mineral wool materials, the airflow resistivity is here set to be in the range from 5000 Nsm^{-4} (5 kNsm^{-4}) to 150000 Nsm^{-4} (150 kNsm^{-4}). In that regard, the airflow resistivity is changed with a step of 5 kNsm^{-4} , or a particular value is taken for this parameter.

In order to compare the predicted and measured results, the absorption coefficient of two samples of a rock mineral wool was measured in the impedance tube. Besides, the airflow resistivity of these two samples was also measured according to the standard ISO 9053-1. The reported value is the average

of measurements undertaken on 9 test samples. The measured airflow resistivities were used as an input to the analyzed models, and the absorption coefficients obtained in this way are compared here with the ones obtained in the measurements.

IV. PREDICTED AND MEASURED ABSORPTION COEFFICIENT

Effects of changing the airflow resistivity on the absorption coefficient predicted by particular model (DB model) are presented in Fig. 1. Smaller values of airflow resistivity, up to 30 kNsm^{-4} , given in Fig. 1.a) lead to more typical absorption coefficient curve where absorption coefficient increases with frequency up to a certain frequency, in this case up to a frequency in the range between 1 kHz and 1.6 kHz. For further increase in frequency, the absorption coefficient has either a dip or remains almost constant.

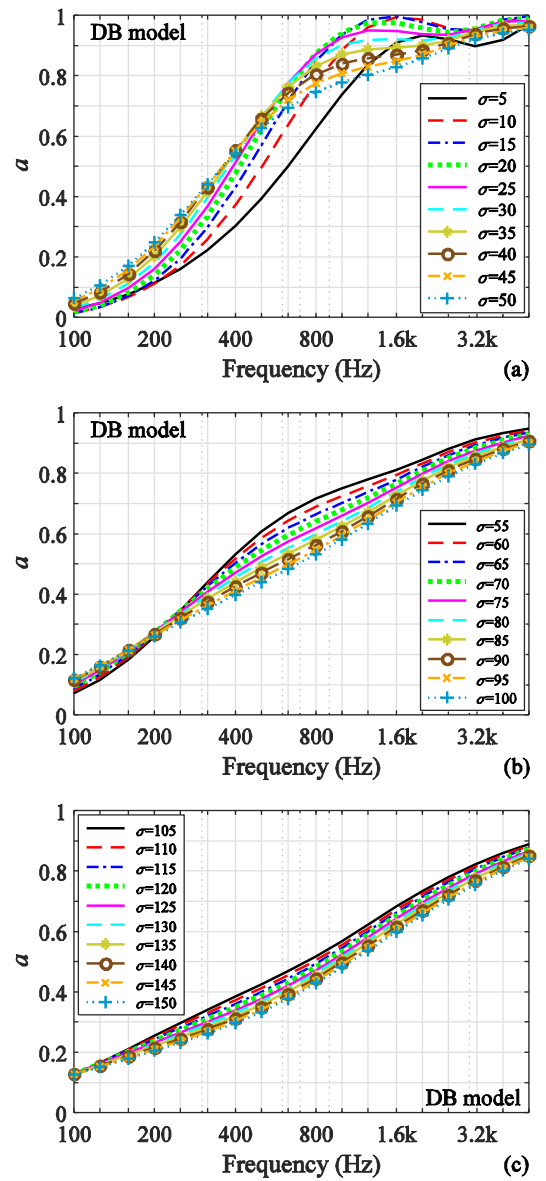


Fig. 1. Absorption coefficients obtained by the DB model changing the values of the airflow resistivity from 5 kNsm^{-4} to 150 kNsm^{-4} with the step of 5 kNsm^{-4} (values of the airflow resistivity in the legend are given in kNsm^{-4}).

For the airflow resistivities in the range from 35 kNsm⁻⁴ to 50 kNsm⁻⁴, the absorption coefficient curve has two parts, the first one with larger slope (up to about 630 Hz), and the second part with smaller slope, above 630 Hz. Here, an increase in the airflow resistivity leads to a decrease in the absorption coefficient at higher frequencies (above 630 Hz). Opposite behavior can be seen at frequencies below 630 Hz.

On the other hand, larger values of the airflow resistivity, especially those greater than 70 kNsm⁻⁴ result in the absorption coefficient curves having almost constant increase of the absorption coefficient with frequency. Here, larger the airflow resistivity, smaller the absorption coefficient at frequencies greater than several hundreds of hertz.

Regarding the interpolating range ($0.01 \leq f/\sigma \leq 1$) where the DB model can be used with confidence, this condition is not satisfied at low frequencies for some values of the airflow resistivity. Thus, at 100 Hz, the requirement is $\sigma \leq 10$ kNsm⁻⁴, which is not satisfied for majority of the airflow resistivities used in Fig. 1. Considering the condition for minimum airflow resistivity, it is required that $\sigma \geq f$, which is always satisfied since the largest frequency used is 5 kHz, and the minimum airflow resistivity is 5 kNsm⁻⁴. Table II summarizes the maximum values of the airflow resistivity satisfying the stated condition at low frequencies.

TABLE II
MAXIMUM VALUES OF THE AIRFLOW RESISTIVITY SATISFYING THE CONDITION ($0.01 \leq f/\sigma$) WHERE THE DB MODEL CAN BE USED WITH CONFIDENCE

f (Hz)	100	125	160	200	250	315	400
σ (kNsm ⁻⁴)	10	12.5	16	20	25	31.5	40

Focus is here on the airflow resistivity values belonging to the range from 20 kNsm⁻⁴ to 60 kNsm⁻⁴ that are often found in the rock mineral wool materials. Fig. 2 presents the absorption coefficients obtained by each of the five analyzed models and airflow resistivity in the above mentioned range with the step of 10 kNsm⁻⁴. With regard to dependence on the airflow resistivity, the absorption coefficient curves can be split in two parts, where the limit between these parts is a frequency between 400 Hz and 630 Hz. For the frequencies below this limit frequency, a larger airflow resistivity gives a larger absorption coefficient. The trend is opposite at frequencies higher than the limit frequency. The noticed trend is present in the results obtained by all five models.

Comparison of the absorption coefficients obtained by different models using the same airflow resistivity is presented in Fig. 3. The results obtained by four models (DB, MG, Wilson and JCA) are rather similar, while only the JCAL model leads to slightly different results, although the trends are the same in the results for all five models. The phrase “trend” is here related to the general shape of the absorption coefficient curve and change of the absorption coefficient values with airflow resistivity. Differences among the results obtained by the analyzed models become slightly smaller with an increase in the airflow resistivity.

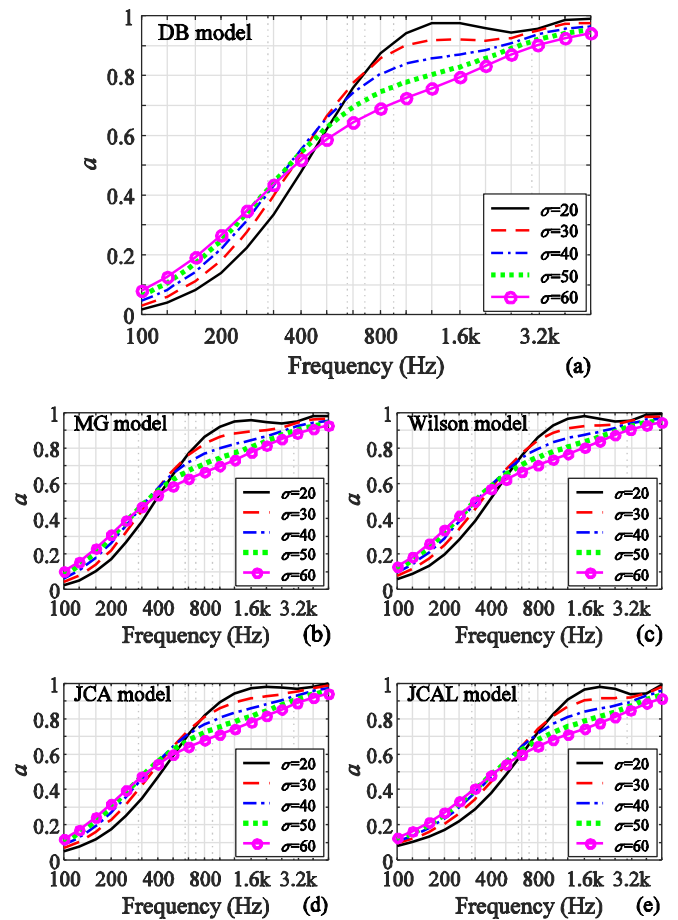


Fig. 2. Comparison of absorption coefficients obtained by a particular model for airflow resistivity in the range from 20 kNsm⁻⁴ to 60 kNsm⁻⁴ with the step of 10 kNsm⁻⁴.

Since the semi-phenomenological models have more input parameters, and only a single set of values is applied here, by changing these input parameters, the obtained absorption coefficient can get different values. This means that the difference between the models shown in Fig. 3 can be changed, and even decreased by choosing other values of the input parameters. This topic will be investigated in the next phase of the research.

When the absorption coefficients obtained by modeling are compared with the ones obtained by the measurements in the impedance tube, different results can be achieved. In some cases, the agreement between the predicted and measured values is better, while in some other cases these values can be rather different. Relatively good agreement between the prediction and measurement is shown in Fig. 4.a), while slightly worse agreement is shown in Fig. 4.b). In the former case, a larger deviation of the predicted absorption coefficient from the measured one is obtained only at three third-octave bands, from 400 Hz to 630 Hz, where the maximum deviation is about 0.3 at 500 Hz. On the other hand, the maximum deviation between the predicted and measured values in Fig. 4.b) is smaller, but the absorption coefficient curves are not coincident in a wider frequency range, from 500 Hz to 2.000 Hz.

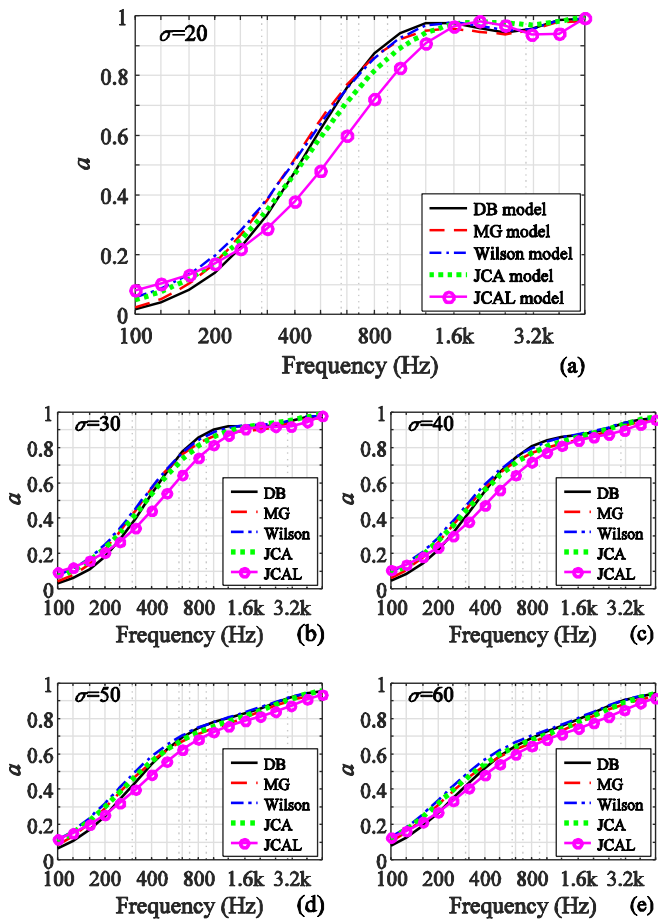


Fig. 3. Comparison of absorption coefficients obtained by all five analyzed models for a particular airflow resistivity in the range from 20 kNsm⁻⁴ to 60 kNsm⁻⁴ with the step of 10 kNsm⁻⁴.

V. CONCLUSION

Different models can be used to predict the absorption coefficient. Some of them called empirical models are based only on a single parameter, the airflow resistivity. Other models called semi-phenomenological use several parameters as an input. The obtained predicted results depend on these parameters heavily. Comparing the results generated by the five analyzed models, it can be concluded that the predicted values are rather similar, having larger differences only for the JCAL model. However, the parameters of this model can be chosen in such a way to give the results closer to other models. The effects of these parameters will be studied in the next phase of the research.

Changing the airflow resistivity in the range from 5 kNsm⁻⁴ to 150 kNsm⁻⁴, significant differences in the absorption coefficient curves are obtained. These differences are related to both shape of the absorption coefficient curve and values of the absorption coefficient. Smaller airflow resistivities (up to 30 kNsm⁻⁴) lead to an absorption curve with shape characteristic for porous materials seen in a number of references. Increase of the airflow resistivity results in reduction of the absorption coefficient at higher frequencies, and the absorption coefficient curve approaches to a curve having a constant increase with frequency.

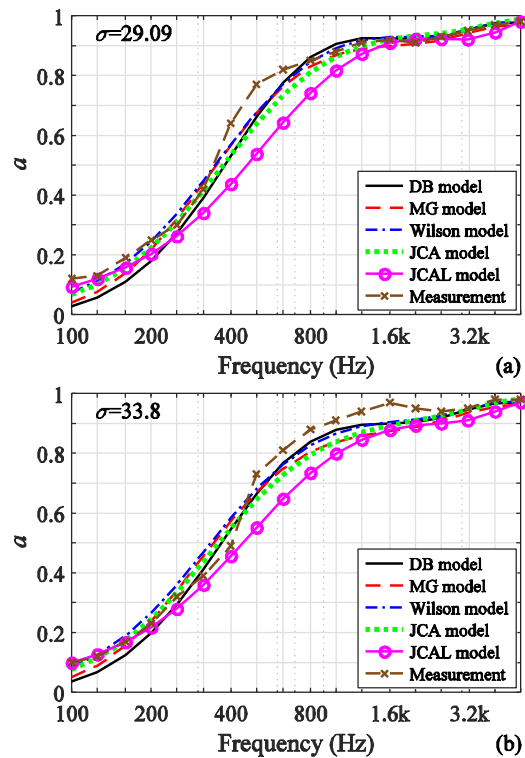


Fig. 4. Absorption coefficients obtained by all analyzed models as well as measurements in the impedance tube for two particular rock mineral wool samples having airflow resistivity of a) 29.090 kNsm⁻⁴ and b) 33.800 kNsm⁻⁴.

ACKNOWLEDGMENT

This work has been partly supported by the Ministry of Science, Technological Development and Innovation of the Republic of Serbia, contract no. 451-03-47/2023-01/ 200102.

REFERENCES

- [1] 43 M. Raj, S. Fatima, N. Tandon, "Prediction of acoustical performance with and without airflow resistivity of fibrous natural materials," in *Recent Dev. Acoust.*, Singapore: Springer, 2021, pp. 149–160.
- [2] 2 M.E. Delany, E.N. Bazley, "Acoustical properties of fibrous absorbent materials," *Appl. Acoust.*, vol. 3, no. 2, pp. 105–116, 1970.
- [3] 3 Y. Miki, "Acoustical properties of porous materials: Modifications of Delany-Bazley models," *J. Acoust. Soc. Japan*, vol. 11, pp. 19–24, 1990.
- [4] 38 K. Ballagh, "The accuracy of methods for predicting sound absorption coefficients," Proc. DAGA 2008, Dresden, Germany, pp. 205–206, 10–13 March, 2008.
- [5] 18 X. Zhu, B.-J. Kim, Q. Wu, "Recent advances in the sound insulation properties of bio-based materials," *BioResources*, vol. 9, no. 1, pp. 1764–1786, 2014.
- [6] 41 D. Oliva, V. Hongisto, "Sound absorption of porous materials – Accuracy of prediction methods," *Appl. Acoust.*, vol. 74, no. 12, pp. 1473–1479, 2013.
- [7] Cox T. J. Cox, P. D'Antonio, *Acoustic Absorbers and Diffusers*, 3rd ed. Boca Raton, Florida, USA: CRC Press, 2017.
- [8] 45 U. Berardi, G. Iannace, "Predicting the sound absorption of natural materials: Best-fit inverse laws for the acoustic impedance and the propagation constant," *Appl. Acoust.*, vol. 115, pp. 131–138, Jan, 2017.
- [9] 48 M. Garai, F. Pompoli, "A simple empirical model of polyester fibre materials for acoustical applications," *Appl. Acoust.*, vol. 66, no. 12, pp. 1383–1398, 2005.
- [10] 39 R. Del Rey, A. Uris, J. Alba, P. Candelas, "Characterization of sheep wool as a sustainable material for acoustic applications," *Materials*, vol. 10, no. 11, pp. 1277–1287, 2017.
- [11] 46 J.-F. Allard, Y. Champou, "New empirical equations for sound propagation in rigid frame fibrous materials," *J. Acoust. Soc. Am.*, vol. 91, no. 6, pp. 3346–3353, 1992.